Full-Wave Analysis of Microstrip Open-End and Gap Discontinuities

ROBERT W. JACKSON, MEMBER, IEEE, AND DAVID M. POZAR, MEMBER, IEEE

Abstract —**A solution is presented for the characteristics of microstrip open-end and gap discontinuities on an infinite dielectric substrate. The exact Green's function of the grounded dielectric slab is used in a moment method procedure, so surface waves as well as space-wave radiation are included. The electric currents on the line are expanded in terms of longitudinal subsectional piecewise sinusoidal modes near the discontinuity, with entire domain traveling-wave modes used to represent incident, reflected, and, for the gap, transmitted waves away from the discontinuity. Results are given for the end admittance of an open-ended line, and the end conductance is compared with measurements. Results are also given for the reflection coefficient magnitude and surface-wave power generation of an open-ended line on substrates with various dielectric constants. Loss to surface and space waves is calculated for a representative gap discontinuity.**

I. Introduction

THIS PAPER DESCRIBES a "full-wave" solution of the open-end and symmetric gap discontinuities in microstrip line. The solution is rigorous in that space-wave radiation and surface-wave generation from discontinuities is explicitly included through the use of the exact Green's function for a grounded dielectric slab. A moment method procedure is used whereby the electric surface current density on the microstrip line is expanded in terms of four different types of expansion modes: one mode represents a traveling wave incident on the discontinuity, another mode represents a traveling wave reflected from the discontinuity, a third represents a traveling wave transmitted through the discontinuity (gap case only), and a number of subsectional (piecewise sinusoidal) modes are used in the vicinity of the discontinuity to model the nonuniform current in that region. The result is a physically meaningful solution in terms of incident, reflected, and transmitted-wave amplitudes, with only a small number of unknown coefficients to solve for (typically four to five for the open-end case and twice that for the gap case). For the open-end case, the complex reflection coefficient can then be determined, as well as an "end admittance," referred to the end of the microstrip line. For the gap, scattering parameters can be determined. In addition, the amount of real power delivered to radiation and surface waves can be calculated. It is assumed that only the fundamental microstrip mode is propagating on the line away from the open end, although higher order mode fields are accounted for in the vicinity of the discontinuity.

Manuscript received January 11, 1985; revised June 3, 1985. This work was supported in part by the Rome Air Development Center, Hanscom Air Force Base, MA, under U.S. Air Force Contracts F19628-84-K-0022 and F49620-82-C-0035.

The authors are with the Department of Electrical and Computer Engineering, University of Massachusetts, Amherst, MA 01003.

Much of the previous work on the open-circuited microstrip line has used quasi-static approximations, with the results of Hammerstad and Bekkadal [1], [2] being widely referenced. Jansen [3] has calculated length extensions for an enclosed microstrip using a spectral-domain method. Lewin [4] used an assumed current distribution to calculate the radiated power from an open line. James and Henderson [5], [6] developed an improved analysis using a variational technique, including surface-wave effects, and compared their results favorably with measurements of the end conductance of an open-ended line on a thin, low dielectric constant substrate. Compared with the present solution, the results of James and Henderson appear to be quite good for such substrates, and their relatively simple expressions are an advantage computationally.

Likewise, the gap has also been analyzed by predominately quasistatic methods [7]–[10], the results of which are used extensively in computer-aided design routines. Fully electromagnetic solutions have been calculated by Jansen and Koster [11] using a spectral-domain method, but their gap is surrounded on four sides by perfect conductors. None of the aforementioned approaches include surface waves and radiation losses.

There were two motivations for the present work. First, the increasing interest in monolithic and millimeter-wave integrated circuits requires rigorous analyses to characterize such microstrip discontinuities on electrically thick, high dielectric constant substrates (such as GaAs, with $\epsilon_r = 12.8$). Quantities such as radiation and surface waves are more important with such substrates than with thin, low dielectric constant substrates. Second, the present work is an ancillary result from the solution to the problem of a microstrip patch antenna on an electrically thick substrate fed by a microstrip line. This problem is also of interest in terms of MMIC design, and may be addressed in the future.

Section II presents the theory of the solution, which is based on the moment method/Green's function solutions for printed dipole and microstrip patch antennas [12], [13]. The propagation constant for the fundamental mode of an infinite microstrip line is also developed in terms of a "full-wave" solution in this section, and the opportunity is taken to dispel a few myths about propagation on microstrip lines. Section III presents results for terminal conductance and the Δl length extension for $\epsilon_r = 2.32$ and 12.8 substrates, and is compared with measurements and calculations from [1] and [6]. Reflection coefficient magnitudes

0018-9480/85/1000-1036$01.00

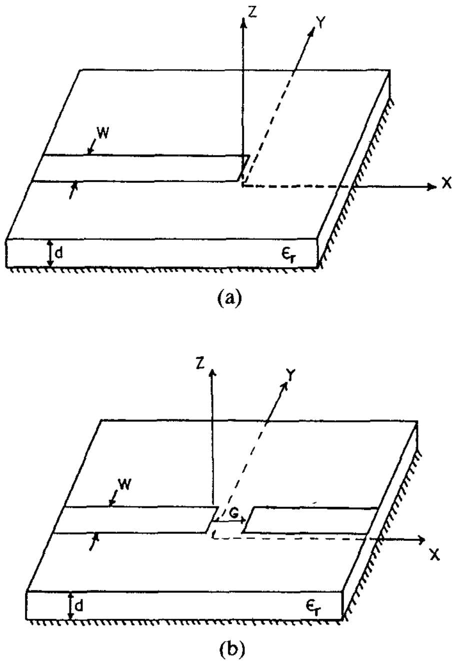

Fig. 1. Geometry of microstrip open-end and gap discontinuities.

and a radiation efficiency e, defined as the ratio of radiated power to radiated plus surface-wave power [13], are plotted versus substrate thickness for $\epsilon_r = 2.55$ and $\epsilon_r = 12.8$. The fraction of incident power launched into surface waves is seen to increase sharply with increasing substrate thickness and/or dielectric constant. Results are also presented for radiation loss at a representative gap discontinuity on $\epsilon_r = 12.8$.

II. Theory

Fig. 1 shows the geometry of the open-end and gap discontinuities in width W. The substrate is assumed infinitely wide in the x- and y-directions, and of thickness d, and relative permittivity ϵ_r. Only $\hat{x}$-directed electric surface currents are assumed to flow on the microstrip line, which, as was found in [14] and other references, is a good approximation when thin lines (with respect to wavelength) are used on substrates of any thickness.

A. Green's Function for the Grounded Dielectric Slab

The canonical building block for the present solution is the plane-wave spectral representation of the grounded dielectric slab Green's function, representing the $\hat{x}$-directed electric field at (x, y, d) due to an $\hat{x}$-directed infinitesimal dipole of unit strength at (x_0, y_0, d). This field can be written as [12]

$$E_{xx}(x, y|x_0, y_0) = -\iint_{-\infty}^{\infty} Q(k_x, k_y) e^{jk_x(x-x_0)} \cdot e^{jk_y(y-y_0)}\, dk_x\, dk_y \quad (1)$$

where

$$Q(k_x, k_y) = \frac{jZ_0}{4\pi^2 k_0} \frac{(\epsilon_r k_0^2 - k_x^2) k_2 \cos k_1 d + jk_1(k_0^2 - k_x^2)\sin k_1 d}{T_e T_m} \sin k_1 d \quad (2)$$

$$T_e = k_1 \cos k_1 d + jk_2 \sin k_1 d$$
$$T_m = \epsilon_r k_2 \cos k_1 d + jk_1 \sin k_1 d$$
$$k_1^2 = \epsilon_r k_0^2 - \beta^2, \qquad \operatorname{Im} k_1 < 0$$
$$k_2^2 = k_0^2 - \beta^2, \qquad \operatorname{Im} k_2 < 0$$
$$\beta^2 = k_x^2 + k_y^2$$
$$k_0 = \omega\sqrt{\mu_0 \epsilon_0} = 2\pi/\lambda_0$$
$$Z_0 = \sqrt{\mu_0/\epsilon_0}. \quad (3)$$

As discussed in [12], the zeros of the T_e, T_m functions constitute surface-wave poles. During the integration in (1), which is done numerically, special care must be given to these pole contributions, and a method for doing this is presented in [12]. The integration in (1) is further facilitated by a conversion to polar coordinates, as described in [12].

B. Propagation Constant of an Infinite Microstrip line

The solution for the open-circuited line requires the propagation constant of an infinitely long microstrip line. It is assumed that the electrical thickness of the substrate is such that only the fundamental microstrip mode propagates. A quasi-static value [2] could be used with reasonable results, but the more rigorous "full-wave" solution involves only a small fraction of the total effort for the open-circuit problem, and so the propagation constant was computed in this manner. The method is very similar to [14].

Consider an infinitely long microstrip line of width W with a traveling-wave current of the form $e^{-jk_e x_0}$, where k_e is the effective propagation constant to be determined. Substituting this current into (1) and integrating over x_0, y_0 yields the electric field at (x, y, d) due to this line source

$$E_{xx}^{l} = -2\pi \iint_{-\infty}^{\infty} Q(k_x, k_y)\delta(k_x + k_e) \cdot e^{jk_x x} e^{jk_y y} F_y(k_y)\, dk_x\, dk_y \quad (4)$$

where F_y is the Fourier transform of the distribution of current in the y-direction, which is, for now, assumed uniform. Thus

$$F_y(k_y) = \frac{2\sin(k_y W/2)}{k_y}. \quad (5)$$

Now, the above electric field must vanish at all points on the microstrip line, since it is assumed to be a perfect conductor. This boundary condition is enforced across the width of the strip by integrating on y over the width. After carrying out the k_x integration, the following characteristic equation for k_e results:

$$\int_{-\infty}^{\infty} Q(k_e, k_y) F_y^2(k_y)\, dk_y = 0. \quad (6)$$

This equation can be solved relatively quickly for k_e using a simple search technique, such as the interval halving method. The characteristic impedance of the uniform line (used later) can also be derived from this solution by computing the voltage between the strip and the ground plane [12]. In the interest of brevity, this derivation is not presented.

Two points of interest regarding propagation on uniform microstrip lines can be inferred from the above solution. First, there exists in the literature (for example, [15] and [16]) the idea that surface-wave modes can be excited by the fundamental mode of the uniform microstrip line. This is false, as can be seen by noting that the fundamental propagation constant k_e (as determined numerically) is always greater than any surface-wave pole β_{sw}. Thus, the integration path of (6) never crosses a surface-wave pole, with the result that no surface-wave power is generated by the uniform line. Discontinuities in the line can, of course, excite surface waves, as can higher order propagating modes.

Second, it is sometimes stated that a uniform microstrip line does not radiate *any* power into space waves. Again, this is false, as a stationary phase evaluation of the field above the substrate due to a uniform line will show far-zone radiated power is generated. As a practical matter, however, this loss to radiation is much less than either conductor loss or dielectric loss.

C. Current Expansion Modes

The method of solution for both the open-circuited microstrip line and the gap basically involves expanding the electric surface current density on the line and formulating an integral equation which can be solved by the method of moments for the unknown expansion currents. The choice of basis functions affects the computational efficiency quite significantly, so a judicious choice is important. We first describe in detail the basis functions for the open end and then describe the modifications needed to compute the gap.

In this formulation, only $\hat{x}$-directed currents are assumed, which should be adequate for lines that are not too wide [14]. Sinusoids, several cycles in length, are used to represent incident and reflected traveling waves of the fundamental microstrip mode, and subsectional (piecewise sinusoidal) modes are used near the open end, to represent currents that do not conform to the fundamental mode. This approach thus differs from a recent solution to the microstrip dipole antenna proximity fed by a microstrip line [17], where subsectional expansion modes were used. We also note that, in contrast to [5], the exciting wave is not assumed to be TEM.

Thus, define an incident electric current of unit amplitude as

$$I^{\mathrm{inc}} = e^{-jk_e x} \tag{7}$$

and a reflected current as

$$I^{\mathrm{ref}} = -Re^{jk_e x} \tag{8}$$

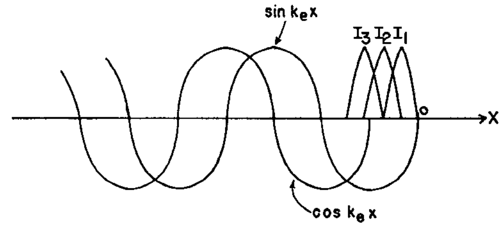

Fig. 2. Layout of expansion modes on the open-ended microstrip line.

where R is the reflection coefficient referenced to the end of the line ($x = 0$). Now, because of the method of numerically integrating (1) [12], it is useful to deal with only real expansion modes; thus, a simple transformation from exponential form to sine and cosine form is made

$$I^{\mathrm{inc}} + I^{\mathrm{ref}} = (1-R)\cos k_e x - j(1+R)\sin k_e x, \qquad x < 0. \tag{9}$$

At $x = 0$, the total electric current must be zero. The sine term of the above current satisfies this condition, but not the cosine term, so the cosine term is truncated at $x = -\pi/2k_e$. Also, both terms are truncated after several cycles. The incident and reflected current components can then be written as

$$I^{\mathrm{inc}} + I^{\mathrm{ref}} = (1-R)f_s(k_e x + \pi/2) - j(1+R)f_s(k_e x) \tag{10}$$

where

$$f_s(u) = \begin{cases} \sin u, & 0 > u > -m\pi \\ 0, & \text{otherwise} \end{cases}.$$

It has been found that choosing the length of the sinusoids to be an integer number of half wavelengths speeds the convergence of the integrals shown in the next section. (Physically, this means that no end charges exist on the lines, as would be the case if the end currents were nonzero.) Typically, the solutions are insensitive to sinusoid length for lengths greater than three or four wavelengths.

Piecewise sinusoidal (PWS) modes are defined starting at the end and working left. These modes can be defined as

$$I_n f_n(x,y) = I_n \frac{\sin k_e(h - |x - x_n|)}{\sin k_e h}, \qquad \text{for } |x - x_h| < h, |y| < W/2 \tag{11}$$

where I_n is the unknown expansion coefficient, h is the half-length of the mode, and x_n is the terminal location, which is chosen as $x_n = -nh$, for $n = 1,2,3,\cdots$. The current is assumed uniform across the strip width. Fig. 2 shows how the various modes are arranged on the microstrip line. Typically convergence is achieved with three or four PWS modes.

D. Integral Equation/Moment Method Solution

An integral equation for the discontinuity is written by enforcing the boundary condition that the total $\hat{x}$ electric field due to all the currents on the line must be zero on the line. Equation (1) then yields

$$\int_{x_0}\int_{y_0}\left[I^{\rm inc}+I^{\rm ref}+\sum_{n=1}^{N} I_n f_n\right]E_{xx}\,dx_0\,dy_0=0,$$
$$\text{for } x<-\infty,\ |y|<W/2 \quad (12)$$

where N is the total number of PWS modes. This equation is enforced by multiplying by $N+1$ weighting or test functions (since there are $N+1$ unknowns), taken here as PWS modes as defined in (11) for $n=1$ to $N+1$, and integrating over x and y. Impedance matrix elements can then be defined as

$$Z_{mn}=\iint_{-\infty}^{\infty} Q(k_x,k_y)F_y^2(k_y)F_{xm}(k_x)F_{xn}^*(k_x)\,dk_x\,dk_y \quad (13)$$

$$Z_{mc}=\iint_{-\infty}^{\infty} Q(k_x,k_y)F_y^2(k_y)F_{xm}(k_x)F_{xc}^*(k_x)\,dk_x\,dk_y \quad (14)$$

$$Z_{ms}=\iint_{-\infty}^{\infty} Q(k_x,k_y)F_y^2(k_y)F_{xm}(k_x)F_{xs}^*(k_x)\,dk_x\,dk_y \quad (15)$$

where F_y is the Fourier transform defined in (5), and F_{xn}, F_{xc}, F_{xs} are Fourier transforms of the mode currents

$$F_{xn}=\int_{x_n-h}^{x_n+h} f_n(x)e^{jk_x x}\,dx \quad (16)$$

$$F_{xs}=\int_{-m\pi/k}^{0}\sin k_e x e^{jk_x x}\,dx \quad (17)$$

$$F_{xc}=\exp\left[-jk_x\pi/(2k_e)\right]F_{xs}. \quad (18)$$

This results in a matrix equation for the unknown coefficients $R, I_1, I_2,\cdots, I_N$. For example, with two PWS modes, $N=2$, and a 3×3 matrix equation results

$$\begin{bmatrix} Z_{11} & Z_{12} & -(Z_{1c}+jZ_{1s})\\ Z_{21} & Z_{22} & -(Z_{2c}+jZ_{2s})\\ Z_{31} & Z_{32} & -(Z_{3c}+jZ_{3s})\end{bmatrix}\cdot\begin{bmatrix} I_1\\ I_2\\ R\end{bmatrix}=\begin{bmatrix} -Z_{1c}+jZ_{1s}\\ -Z_{2c}+jZ_{2s}\\ -Z_{3c}+jZ_{3s}\end{bmatrix}. \quad (19)$$

Note that the above testing procedure only enforces (12) near the open end, where the testing modes are located. Farther away from the end (but still much greater than $-m\pi/k_e$), (12) is automatically satisfied since then the line looks locally as if it were infinitely long, and (6) implies that the E_x field is near zero. In other words, Z_{nc} and Z_{ns} quickly approach zero as n increases.

E. Surface-Wave Power

With the above formulation, the reflection coefficient of the open-circuited microstrip line can be found. Since the termination is not an *ideal* electrical open circuit, the reflection coefficient magnitude is always less than unity, implying that some incident power is lost to radiation of space and surface waves. In addition, an end admittance Y can be defined using the characteristic impedance Z_0 of the line. Thus

$$Y=\frac{1-R}{Z_0(1+R)}. \quad (20)$$

In order to quantify the separation of the total power loss into space-wave radiation and surface-wave excitation, an efficiency is defined as in [13]

$$e=\frac{P_{\rm rad}}{P_{\rm rad}+P_{\rm sw}} \quad (21)$$

where $P_{\rm rad}$ is the power lost to space waves and $P_{\rm sw}$ is the power lost to surface waves. This efficiency was originally defined for printed antennas [13] and is used here in the interest of consistency. The powers in (21) are found as follows:

$$P_{\rm rad}+P_{\rm sw}={\rm Re}\left\{\sum_{i=1}^{N+2}\sum_{j=1}^{N+2} I_i Z_{ij} I_j^*\right\} \quad (22)$$

$$P_{\rm sw}={\rm Re}\left\{\sum_{i=1}^{N+2}\sum_{j=1}^{N+2} I_i Z_{ij}^{sw} I_j^*\right\} \quad (23)$$

where

$$I_i=\begin{cases} I_i, & \text{for } 1\leqslant i\leqslant N\\ (1-R), & \text{for } i=N+1\\ -j(1+R), & \text{for } i=N+2\end{cases} \quad (24)$$

and Z_{ij} is an impedance matrix element with indices i, j for $i, j\leqslant N$, $i, j=c$ for $i, j=N+1$, and $i, j=s$ for $i, j=N+2$. The Z_{ij}^{sw} elements represent only the surface-wave contribution of the Z_{ij} elements, as computed from the residues of the surface-wave poles [12].

F. Gap Formulation

It is not difficult to modify the formulation for the open end in order to compute gap-discontinuity parameters. The configuration is shown in Fig. 1(b) with a gap G between the input and output microstrip lines. To analyze this discontinuity, three entire domain modes are used to represent incident, reflected, and transmitted currents. In addition to $I^{\rm inc}$ and $I^{\rm ref}$, we therefore add

$$I^{\rm tr}=Te^{-jk_e(x-G)} \quad (25)$$

which is then modified in a manner similar to (9) and (10) to eliminate current discontinuities and to impose a finite length. This results in

$$I^{\rm tr}=T\left[-g\left(k_e[x-G]-\frac{\pi}{2}\right)-jg\left(k_e[x-G]\right)\right] \quad (26)$$

where

$$g(u)=\begin{cases}\sin u, & 0<u<m\pi\\ 0, & \text{otherwise}\end{cases}$$

which is then placed, with $I^{\rm inc}$ and $I^{\rm ref}$, in (12) along with additional piecewise sinusoidal modes (eq. (11)). Piecewise modes will now exist at $x_n=-nh$ and at $x_n=nh+G$ for

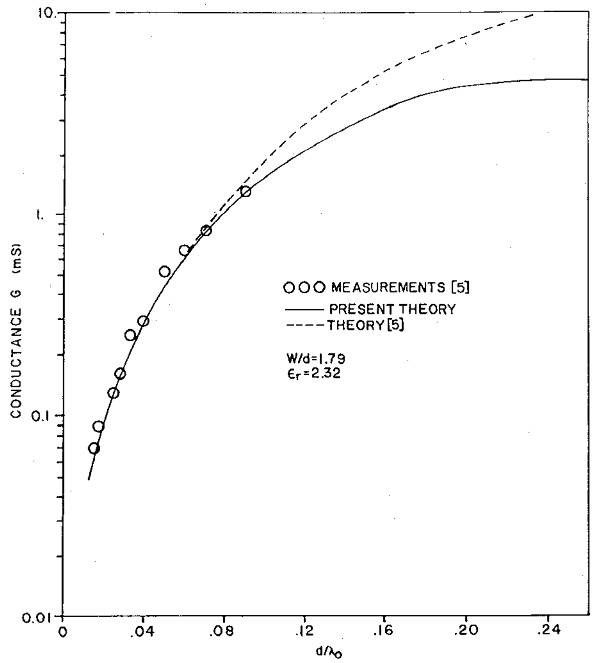

Fig. 3. Comparison of calculated end conductance of an open-circuit microstrip line compared with measurements and calculations of [5].

$n = 1, 2, \cdots, N$. This gives a total of $2N$ piecewise modes. Equation (12) has thus been modified such that R, T, and I_n are $2N+2$ unknowns for which one can solve once (12) has been tested with $2N+2$ piecewise testing functions. The remaining formulation is analogous to (13)–(19). We note that in computing the impedance matrix elements there are several redundancies due to reciprocity and due to the physical symmetry of the gap configuration. Making use of these redundancies considerably reduces computation time.

III. Results

Fig. 3 shows the terminal conductance of an open-circuited microstrip line as computed by this theory and compared with the measurements of [5] and calculations of [5] and [6]. The agreement of both theories and the measured data is good for substrate thickness up to about $0.1\lambda_0$, while the theories depart slightly above this value. In contrast to this theory, James and Henderson assume a TEM parallel-plate mode as an excitation. For thicker, higher dielectric constant substrates, their assumption is questionable and the two theories may diverge more readily. Note the trend that, as the substrate thickness increases, the termination looks less like an ideal open circuit.

Fig. 4(a) and (b) shows the reflection coefficient magnitude and efficiency e versus substrate thickness for $\epsilon_r = 2.55$, and various microstrip line widths. The efficiency e is practically independent of widths. Observe from Fig. 4(a) that the reflection coefficient magnitude drops well below unity for substrate thicknesses greater than a few hundreths of a wavelength, and is smaller for wider strips, as would be expected. The efficiency data of Fig. 4(b) shows that very little of the total power loss is caused by surface-wave

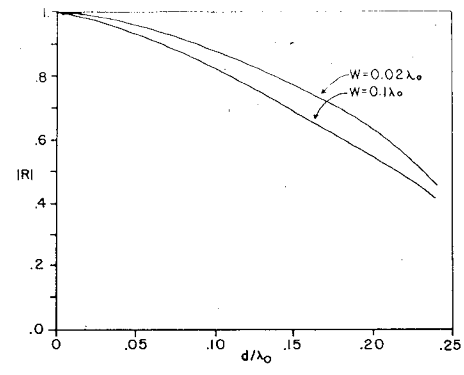

(a)

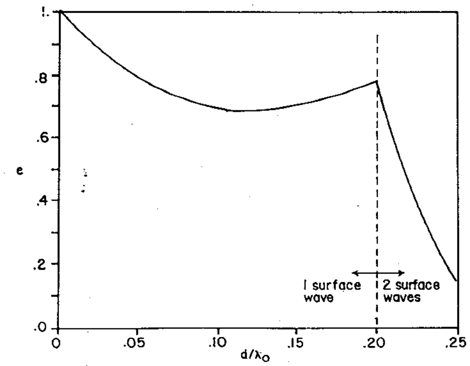

(b)

Fig. 4. (a) Reflection coefficient magnitude and (b) efficiency for an open-circuit microstrip line on an $\epsilon_r = 2.55$ substrate.

excitation when the substrate is thin, but that the surface-wave power increases (e decreases) for thicker substrates, with a cusp in the data at the cutoff point of the TE_1 surface-wave mode. This curve is very similar to that obtained for printed antennas [12], [18]. Fig. 5(a) and (b) shows corresponding data for a substrate with $\epsilon_r = 12.8$. It can be seen that the reflection coefficient magnitude drops off more rapidly with increased permittivity, and that significantly more power is launched into surface waves, for a given substrate thickness.

The data given in Figs. 3 and 4 allow one to determine the amount of power loss and the amount of surface-wave power generation of an open-circuit line. For example, assume that $1w$ of power is incident on an open microstrip line of width $0.1\lambda_0$ on a GaAs ($\epsilon_r = 12.8$) substrate $0.04\lambda_0$ thick. Then, from Fig. 5(a) and (b), $|R| = 0.96$ and $e = 0.53$, so there is $0.922w$ reflected on the line, $0.0416w$ delivered to space-wave radiation, and $0.0368w$ delivered to surface waves.

For MIC design, an open-circuit microstrip line is often modeled as having a reflection coefficient with unit magnitude and a phase accounted for by a length extension $\Delta l/d$. When radiation loss occurs, a conductance in parallel with a length extension is necessary, yielding

$$YZ_0 = GZ_0 + j\tan(k_e \Delta l) \quad (27)$$

where Y is given in (20). Fig. 6 gives normalized end conductance for common microstrip parameters on a Gal-

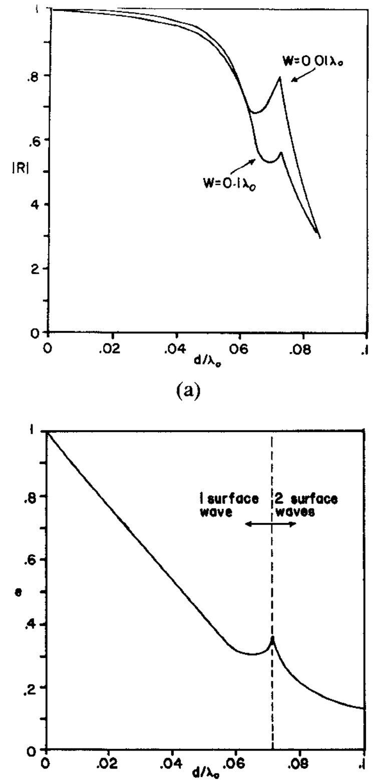

Fig. 5. (a) Reflection coefficient magnitude and (b) efficiency for an open-circuit microstrip line on an $\epsilon_r = 12.8$ substrate.

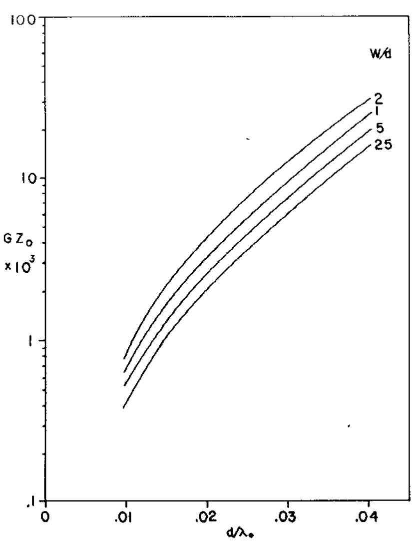

Fig. 6. Normalized end conductance for several common microstrip parameters on $\epsilon_r = 12.8$.

lium Arsenide substrate. For lossless cases, the length extension has been computed by quasi-static analysis [1], [2], as well as other methods [3], [5]. In contrast to the end conductance and reflection coefficient magnitude, we have found the length extension to be much more sensitive to the number of expansion modes, current distribution across the microstrip line, and truncation of the integrations in (13)–(15), especially for thin substrates. Instead of a uni-

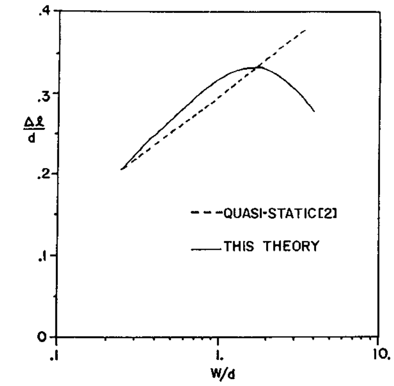

Fig. 7. Calculated length extension of an open-circuit microstrip line compared with quasi-state theory [2] on a substrate with $\epsilon_r = 12.8$, $d = 0.02\lambda_0$.

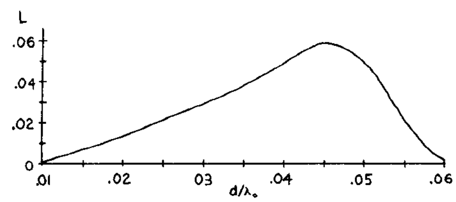

Fig. 8. Loss for a microstrip gap with $\epsilon_r = 12.8$, $G = 0.2d$, $w = 2.5d$.

form current distribution with respect to y, we found that a current distributed to enforce the edge condition

$$I^{\text{inc}}, I^{\text{ref}} \propto \frac{1}{\sqrt{1-(2y/w)^2}} \tag{28}$$

gave better agreement with quasistatic results in the thin substrate limit. Fig. 7 presents calculated results for the length extension using this theory and the quasi-static result [2]. Good agreement occurs for narrow lines but not for lines greater than two substrate thicknesses. Based on this result and on results with substrates having smaller dielectric constants, we conclude that the simple transverse current distribution assumed in (28) will give a reasonable length extension result for widths less than an eighth of a wavelength in the dielectric. For precise length extension calculations, or for wider microstrip lines, a more complicated transverse current distribution is necessary. In this paper, our calculation of length extension is primarily to help validate the less sensitive conductance calculations.

For the gap, we have calculated total power loss due to the combination of surface-wave and space-wave radiation by computing

$$L = 1 - |R|^2 - |T|^2.$$

In Fig. 8, we plot this quantity versus substrate electrical thickness for a representative configuration on Gallium Arsenide. Loss increases, peaks, and then decreases as frequency increases. The decrease occurs due to the fact that a gap, intuitively considered as a series capacitance, looks like a series short at high frequencies and thus like less of a radiation-producing discontinuity. This loss data is insensitive to the distribution of current in the transverse direction. We have calculated circuit models for a gap using this method and found models which roughly agree with quasi-static models but which are somewhat sensitive to transverse current distribution. For very accurate calculation of gap and fringing capacitances, a higher degree of modal approximation is desirable. Investigations of this type are underway.

IV. Conclusion

A full-wave analysis has been presented for the problems of microstrip open-end and gap discontinuities. For the open end, the reflection coefficient, radiated power, and surface-wave power have been calculated and compared with previous calculations and measured data, when available. Plots of end conductance and length extension have been presented for a high dielectric substrate. Loss at a gap discontinuity has also been calculated. This type of analysis should aid in the design of microwave integrated circuits, particularly for higher frequencies and high dielectric constant substrates. Similar analysis can be used to characterize more complicated microstrip discontinuities.

References

[1] E. O. Hammerstad and F. Bekkadal, "Microstrip handbook," ELAB Rep. STF44A74169, University of Trondheim, 1975.

[2] K. C. Gupta, R. Garg, and I. J. Bahl, *Microstrip Lines and Slotlines*. Dedham, MA: Artech House, 1979.

[3] R. Jansen, "Hybrid mode analysis of end effects of planar microwave and millimeterwave transmission lines," *Proc. Inst. Elec. Eng.*, vol. 128, pt. H. pp. 77–86, Apr. 1978.

[4] L. Lewin, "Radiation from discontinuities in stripline," *Proc. Inst. Elec. Eng.*, vol. 107C, pp. 163–170, Feb. 1960.

[5] J. R. James and A. Henderson, "High frequency behavior of microstrip open-circuit terminations," *IEE J. Microwave Opt. Acoust.*, vol. 3, pp. 205–211, Sept. 1979.

[6] J. R. James, P. S. Hall, and C. Wood, *Microstrip Antenna Theory and Design*. London: Peter Peregrinus, 1981.

[7] M. Maeda, "An analysis of gaps in microstrip transmission lines," *IEEE Trans. Microwave Theory Tech.*, vol. MTT-20, pp. 390–396, June 1972.

[8] P. Benedek and P. Silvester, "Equivalent capacitances for microstrip gaps and steps," *IEEE Trans. Microwave Theory Tech.*, vol. MTT-20, pp. 729–733, Nov. 1972.

[9] Y. Rahmat-Samii, T. Itoh, and R. Mittra, "A spectral domain analysis for solving microstrip discontinuity problems," *IEEE Trans. Microwave Theory Tech.*, vol. MTT-24, pp. 372–378, Apr. 1984.

[10] A. Gopinath and C. Gupta, "Capacitance parameters of discontinuities in microstrip lines," *IEEE Trans. Microwave Theory Tech.*, vol. MTT-26, pp. 831–836, Oct. 1978.

[11] R. Jansen and N. Koster, "A unified CAD basis for the frequency dependent characterization of strip slot and coplanar MIC components," in *Proc. 11th Eur. Microwave Conf.* (Amsterdam), 1981, pp. 682–687.

[12] D. M. Pozar, "Input impedance and mutual coupling of rectangular microstrip antennas," *IEEE Trans. Antennas Propagat.*, vol. AP-30, pp. 1191–1196, Nov. 1982.

[13] D. M. Pozar, "Considerations for millimeter wave printed antennas," *IEEE Trans. Antennas Propagat.*, vol. AP-31, pp. 740–747, Sept. 1983.

[14] T. Itoh and R. Mittra, "Spectral-domain approach for calculating the dispersion characteristics of microstrip lines," *IEEE Trans. Microwave Theory Tech.*, vol. MTT-21, pp. 496–499, July 1973.

[15] C. P. Hartwig, D. Masse, and R. A. Pucel, "Frequency dependent behavior of microstrip," in *1968 G-MTT Int. Symp. Dig.*, pp. 11–116.

[16] I. J. Bahl and D. K. Trivedi, "A designer's guide to microstrip line," *Microwaves*, pp. 174–182, May 1977.

[17] P. B. Katehi and N. G. Alexopoulos, "On the modeling of electromagnetically coupled microstrip antennas—The printed strip dipole," *IEEE Trans. Microwave Theory Tech.*, this issue, pp. 1029–1035.

[18] P. B. Katehi and N. G. Alexopoulos, "On the effect of substrate thickness and permittivity on printed circuit dipole properties," *IEEE Trans. Antennas Propagat.*, vol. AP-31, pp. 34–39, Jan. 1983.

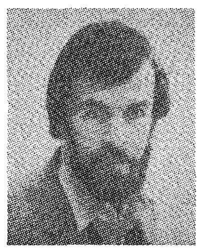

Robert W. Jackson (M'82) was born in Boston, MA, on October 18, 1952. He received the B.S. (1975) and Ph.D. (1981) degrees in electrical engineering from Northeastern University in Boston, MA. His thesis was on nonlinear plasma interactions in the Earth's bow shock.

From 1981 to 1982, he was an Assistant Professor at Northeastern University. Since 1982, he has been on the faculty of the Department of Electrical and Computer Engineering at the University of Massachusetts, Amherst, where he is a member of the Microwave and Electronics Laboratory. His research interests include numerical electromagnetics applied to millimeter-wave integrated circuits and active microwave and millimeter-wave circuit design.

David Pozar (S'74–M'80) was born in Pittsburgh, PA, on January 25, 1952. He received the B.S.E.E. and M.S.E.E. degrees from the University of Akron, Akron, OH, in 1975 and 1976, respectively, and the Ph.D. degree from Ohio State University, Columbus, OH, in 1980. He is currently an Assistant Professor in the Department of Electrical and Computer Engineering at the University of Massachusetts, Amherst, MA.

His research involves the analytical, numerical, and experimental study of printed antennas and phased arrays, and related problems in applied electromagnetics. He is currently an Associate Editor for the IEEE Transactions on Antennas and Propagation. In 1984, he received an NSF Presidential Young Investigator Award, as well as the "Keys to the Future" Award from the IEEE Antennas and Propagation Society.